Feasibility Study of a Partial Gyro-Free Inertial Navigation System Mounted on a Ground Robot*

Hadar Zemer, Reut Sarel and Itzik Klein

***Abstract*— Gyro-free Inertial Navigation System (GFINS) uses only linear accelerometers in order to determine the linear and angular acceleration vectors. For ground robot applications, such a system is redundant and adds unnecessary errors of irrelevant accelerometers. To circumvent this, a partial GFINS configuration is proposed. In the partial configuration only accelerations relevant for two-dimensional ground navigation are employed. A demonstration of the advantages of a partial system compared to the redundant system is provided. The comparison is made using quality factor calculations, simulation and field experiments.**

I. INTRODUCTION

Inertial Navigation System (INS) is a system which calculates the position, velocity and orientation of a body by measuring linear accelerations and angular velocities. In its classical configuration, the INS consist of three orthogonal accelerometers and gyroscopes which provide measurements for the navigation state calculations [1].

The transition to sensors production using MEMS technology enables the construction of smaller INSs at low cost, sometimes at the price of system performance. With technology progress, MEMS accelerometers are capable of maintaining tactical accuracy, while currently MEMS gyroscopes technology is still striving for better accuracy.

A possible solution to the performance problem of MEMS gyroscopes is the use of a gyro-free system, known as all accelerometer configuration or gyro-free INS (GFINS) [2, 3]. In such system, instead of three orthogonal gyroscopes, N linear accelerometers are used to calculate both linear and angular acceleration vectors and thereby functioning as a regular INS [4]. However, there are several errors that origin in the various calculations, and an additional integration is required to obtain the angular velocity vector [5]. In addition, GFINS precision is greatly influenced by the system configuration, that is, the number of the accelerometers and their location [6]. Recently, a state-of-the-art literature review of GFINS and a discussion about its architecture relative to the classical INS architecture was made in [7].

A general rigid-body moving in a three-dimensional space has six degrees of freedom (DoF) – three for translation and three for orientation. Using three linear accelerations and three angular accelerations, the 6 DoF of the rigid body can be determined [8]. When considering ground robot navigation, the general 6 DoF can be reduced to 3DoF - linear translation in x and y axes (for horizontal position propagation), and orientation only in z axis (for heading angle calculation).

To that end, in this paper we propose a partial GFINS configuration that is capable of determining 3 DoF, suitable for ground robot navigation. We present an analysis of several possible GFINS configurations and choose an appropriate one based on quality factors analysis. Using the chosen configuration, reduced GFINS equations of motion are derived. Simulation and field experiments show the benefit of using the partial GFINS architecture over a regular (redundant, in this case) GFINS architecture for ground robot navigation.

The rest of the paper is organized as follow: Section 2 and 3 present the GFINS equations for the redundant and partial systems, respectively. In section 4 different accelerometers' configurations are compared in terms of quality factors. Section 5 introduces the results of Monte Carlo simulations and analysis of the field experiments for the redundant versus the partial configuration. The last section – section 6 includes the summary and conclusions.

II. GFINS EQUATIONS OF MOTION

We follow [9] for the presentation of the GFINS equations of motion. GFINS can be characterized by a configuration matrix that is determined by the number of the accelerometers and their location:

$$H = \begin{pmatrix} (\mathrm{r}_1 \times d_1)^T & \vdots & d_1^T \\ \vdots & \vdots & \vdots \\ (\mathrm{r}_N \times d_N)^T & \vdots & d_N^T \end{pmatrix}_{N\times 6} \quad (1)$$

where r_i is the position vector of accelerometer i in respect to the origin, as shown in the GFINS configurations

* Research supported by CRML lab, Electrical Engineering, Technion – Israel Institute of Technology.

Hadar Zemer Author is with Technion – Israel Institute of Technology, Haifa, Israel, E-mail: smoreno@campus.technion.ac.il

Reut Sarel Author is with Technion – Israel Institute of Technology, Haifa, Israel, E-mail: reutdin@campus.technion.ac.il

Itzik Klein Author is with Technion – Israel Institute of Technology, Haifa, Israel, E-mail: iklein@technion.ac.il

figures in appendix A, and d_i is the direction vector in which accelerometer *i* measures the linear acceleration.

Using the system's matrix (1) and the measurements readings from the accelerometers the specific force and angular acceleration vectors are given by:

$$\begin{bmatrix} \dot{\omega} \\ f \end{bmatrix} = \begin{bmatrix} H_{\dot{\omega}} \\ H_a \end{bmatrix} \left(Y - M \right) \tag{2}$$

where,

$\dot{\omega}$ is the angular acceleration vector, f is the specific force vector calculated at the origin of the GFINS configuration. Given the local gravity vector *g*, the linear acceleration *a* can be found by

$$a = f + g \tag{3}$$

Using the configuration matrix (1), $H_{\dot{\omega}}$ and H_a are sub matrices of the pseudo inverse matrix *H*:

$$\begin{bmatrix} H_{\dot{\omega}} \\ H_a \end{bmatrix} = \left(H^T H \right)^{-1} H^T \tag{4}$$

Y is the measurements vector of all accelerometers in the configuration:

$$Y = \begin{bmatrix} f_1 \\ \vdots \\ f_N \end{bmatrix}_{N \times 1} \tag{5}$$

M is a matrix related to the angular velocity given by

$$M = \begin{bmatrix} {d_1}^T \Omega_{ib}^{b\,2} r_1 \\ \vdots \\ {d_N}^T \Omega_{ib}^{b\,2} r_N \end{bmatrix}_{N \times 1} \tag{6}$$

where Ω_{ib}^b is the skew-symmetric form of the angular velocity vector:

$$\Omega_{ib}^b = \begin{pmatrix} 0 & -\omega_z & \omega_y \\ \omega_z & 0 & -\omega_x \\ -\omega_y & \omega_x & 0 \end{pmatrix} \tag{7}$$

Using the specific force and angular acceleration vectors (2) and assuming that the Earth turn rate can be neglected, the position and velocity of a ground robot can be calculated according to the following equations [1]:

$$\dot{p} = v \tag{8}$$

$$\dot{T}_b^n = T_b^n \Omega_{ib}^b \tag{9}$$

$$\dot{v} = T_b^n f_{ib}^b + \begin{bmatrix} 0 & 0 & g \end{bmatrix}^T \tag{10}$$

where,

p is the position of the body, *v* is the linear velocity of the body, and T_b^n is the transformation matrix between the body and navigation frames for a ground robot determined only using the heading angle and given by

$$T_b^n = \begin{pmatrix} \cos\psi & -\sin\psi & 0 \\ \sin\psi & \cos\psi & 0 \\ 0 & 0 & 1 \end{pmatrix} \tag{11}$$

III. PARTIAL GFINS

In order to derive the partial GFINS equations of motion, first a partial system configuration matrix H_{2D} is defined by removing the accelerometers that are not relevant to the ground navigation, i.e. the accelerometers with sensitivity axis in *z*-axis direction. Next, only columns 3, 4 and 5 from (1) which correspond to the angular acceleration in *z*-axis and the specific forces in *x* and *y* axes are used. In addition, using the fact that the number of relevant accelerometers is now reduced to N' (N'<N), the new system configuration matrix H_{2D} is:

$$H_{2D} = \begin{pmatrix} \left(r_1 \times d_1 \right)_z & \vdots & d_{1_x} & d_{1_y} \\ \vdots & \vdots & \vdots & \vdots \\ \left(r_{N'} \times d_{N'} \right)_z & \vdots & d_{N'_x} & d_{N'_y} \end{pmatrix}_{N' \times 3} \tag{12}$$

For the ground robot 2D navigation, the angular velocity vector in its skew-symmetric form is reduced from (7)

$$\Omega_{ib_{2D}}^b = \begin{pmatrix} 0 & -\omega_z \\ \omega_z & 0 \end{pmatrix} \tag{13}$$

The corresponding acceleration in the navigation frame is:

$$\dot{v}_{2D} = T_{b\ 2D}^n f_{ib}^b \tag{14}$$

And, using (11), the transformation matrix between the body and navigation frames for a ground robot is:

$$T_{b\ 2D}^n = \begin{pmatrix} \cos\psi & -\sin\psi \\ \sin\psi & \cos\psi \end{pmatrix} \tag{15}$$

IV. Configuration Selection for Robot Navigation

Several GFINS configurations are considered. They differ from each other by the number of accelerometers and their location on the robot. For each configuration both the redundant and the partial GFINS were examined using quality factors. The configuration selection is highly significant. Thus, we examine several different quality factors in order to determine which yields the smallest error measure.

A. Quality Factors

The comparison between the different configurations is done by comparing several quality factors that are calculated on the system's matrix given in (1) for each configuration. We employ the same quality factors as in [8].

The first quality factor is the condition number. Solving the system equations involves inverting the system matrix H. A small condition number $\kappa(H)$ indicates low effect of errors on the system accuracy [10].

The other factors are based on dilution of precision (DOP). The DOP measures relate to the effect of the system geometry on its accuracy. Geometric Dilution of Precision (GDOP) is defined as

$$GDOP(H) \triangleq \sqrt{Tr(H^T H)^{-1}} \qquad (16)$$

where H is defined in (1) or in (12) (for partial GFINS). Another two DOP values can be defined by

$$\dot{\omega}DOP(H) \triangleq \sqrt{Tr(H_{\dot{\omega}}{}^T H_{\dot{\omega}})^{-1}} \qquad (17)$$

$$aDOP(H) \triangleq \sqrt{Tr(H_a{}^T H_a)^{-1}} \qquad (18)$$

These values indicate the effectiveness of the system geometry on the angular accelerations (17) and specific force (18) calculation accuracy.

Seven configurations are examined based on the configurations suggested in [11]. For each configuration, both the redundant (3D) and partial (2D) GFINS configurations are analyzed. The quality factors values are shown in the bellow table. The configuration schemes appear in appendix A.

TABLE 1: Quality Factors Comparison of Seven GFINS Configurations

No.		***K(H)***	***GDOP***	***$\dot{\omega}$DOP***	***aDOP***
1	3D	1.2	1.6	1.2	1
	2D	1.2	1.1	0.7	0.8
2	3D	2.5	1.4	0.8	1
	2D	1.4	0.9	0.4	0.8
3	3D	1	1.7	1.2	1.2
	2D	1	1.2	0.7	1
4	3D	2.2	1.8	1.2	0.9
	2D	1.9	1.1	0.7	0.7
5	3D	1.4	1.6	1.3	1
	2D	1	1	0.6	0.8
6	3D	1.7	1.1	0.7	0.7
	2D	1	0.7	0.4	0.6
7	3D	1.5	1.4	1.1	0.9
	2D	1.2	0.9	0.6	0.7

As seen in the table, all partial configurations demonstrate same or lower (better performance) quality factors than the corresponding redundant configuration. This demonstrates that eliminating the redundant accelerometers eliminates their errors as well, and therefore reduces the errors significantly.

B. Chosen Configuration

The chosen configuration is configuration number 7. This configuration yields good quality factors values (compared to the other examined configurations) while meets with the experimental system restrictions (number of analog outputs, etc.). The accelerometers in this configuration are arranged in three triads on a circle with radius d and one triad located on the *z*-axis, as shown in Figure 1.

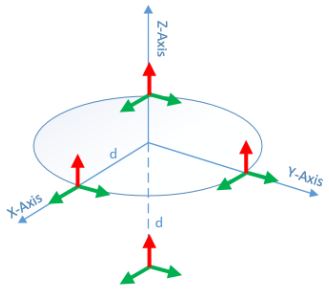

Figure 1. 12 accelerometers configuration. 9 are arranged in triads on a circle within radius d. Another triad is on the *z*-axis at distance d from the origin. The red arrows are accelerometers which are not used in the partial GFINS

V. Results

As shown in the previous section using the quality factor comparison, a partial configuration is expected to yield smaller errors. In this part, this claim is validated by simulation and field experiment. We examine the errors of each configuration in different scenarios.

A. Simulation

The simulations performed were Monte Carlo simulations and are presented for two scenarios: stationary conditions and constant velocity in a straight-line trajectory.

The data from the accelerometers is examined for the two systems. The first is the redundant system that uses the data

from all the accelerometers and the second is the partial system that uses only part of the accelerometers' data.

TABLE 2: SIMULATION RESULTS SUMMARY– ERRORS (IN METERS)

	axis	*Partial configuration*	*Redundant configuration*
Stationary conditions	X	0.7	11.6
	Y	0.8	9.8
Constant velocity	X	0.8	11.1
	Y	0.8	11.2

As can be seen from the simulation results in Table 2, the partial configuration yields smaller errors, by 1 to 2 orders of magnitude.

B. Field Experiment

In this part we present the results of the field experiment using a ground robot. The robot of the type corobot appears in Figure 2.

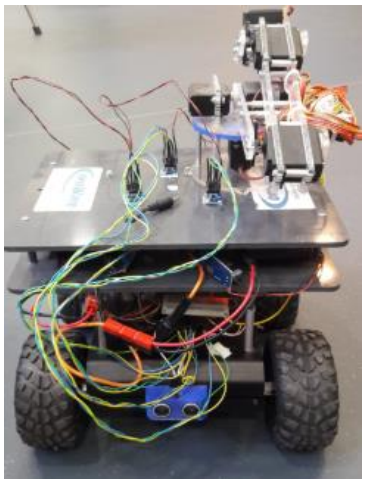

Figure 2. The experiment system – the configuration described in figure 1. is mounted on the robot.

The robot is controlled by an Arduino controller and gets instructions from a remote control. The accelerometers' readings are saved on an SD card using the Arduino controller.

The same two scenarios were examined: stationary conditions and constant velocity.

In order to decrease the errors of the accelerometers we used two methods. First, we used several accelerometers in the same direction that should measure the same acceleration. By averaging the measurements of different accelerometers, the error reduces. Second, we calibrated the accelerometers to eliminate the amplification error in all 3 axes as well as bias error which changes with system reset [12].

Figure 2 shows the position error, of both the partial and full configurations, obtained using the ground robot. As can be seen, the position error of the reduced configuration is much smaller. The error is still quite large due to the performance of the accelerometers we used.

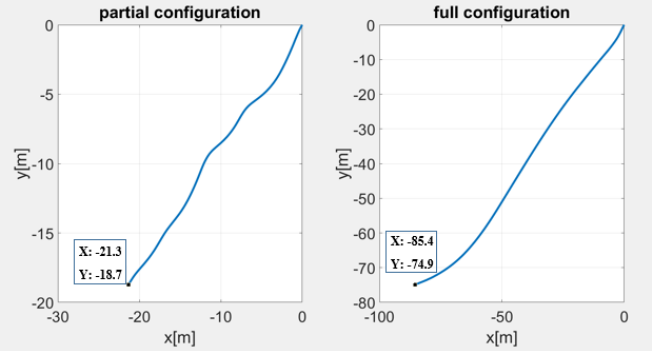

Figure 3. Position error for a stationary scenario using the designed GFINS configuration mounted on the ground robot

Figure 3 describes a constant velocity scenario with an arbitrary heading angle. The robot travelled for distance of ~7 meters during ~17 seconds. It can be seen that the redundant configuration yields larger errors than the partial configuration by an order of magnitude. In addition, the curve of the partial configuration fits the profile of constant velocity, as oppose to the redundant configuration.

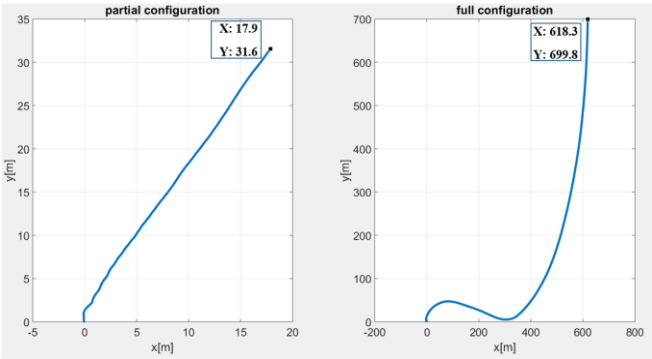

Figure 4. Position error for a constant velocity scenario using the designed GFINS configuration mounted on the ground robot

The following table summarizes the position errors calculated in the different scenarios.

TABLE 3: FIELD EXPERIMENT RESULTS SUMMARY – ERRORS (IN METERS)

	axis	*Partial configuration*	*Redundant configuration*
Stationary conditions	X	21.3	85.4
	Y	18.7	74.9
Constant velocity	X	15.3	615.7
	Y	24.7	693

The errors in constant velocity scenario are much larger than in stationary conditions for the redundant GFINS configuration. This is attributed to the fact that the robot accelerated to obtain its desired constant velocity and as a result scale and misalignment error become more dominant. However, in the partial configuration the same error level

was achieved, and this error is much lower compared to the redundant configuration.

The higher errors in compare to the simulation can origin from the difference in the sampling frequency which was slower. Higher sampling frequency as used in the simulation would result in lower errors, hence better performance.

VI. Summary and Conclusions

In this paper we examined the feasibility of implementing a partial GFINS configuration for ground robot navigation. First, a comparison of quality factors was made on seven GF configurations. After deriving the partial GFINS equations of motion, simulation and field experiments were used to evaluate the proposed approach. We demonstrated that the partial configuration yields smaller errors compared to the redundant configuration in both simulation and field experiments. The advantages of the partial configuration are noticeable: it yields smaller errors compared to the redundant configuration and includes less accelerometers, hence can be implemented at lower cost.

We still see significant errors due to low cost and inaccurate accelerometers used in this study. These errors were handled by calibrations, but in order to minimize the errors additional calibrations are needed.

Additional research in partial GFINS can include the investigation of more suitable configurations that could give more accurate system and experiments in other dynamics.

Appendix A

Herein we describe all GF configurations examined in the paper. In all figures the red arrows are accelerometers which are not used in the partial GFINS.

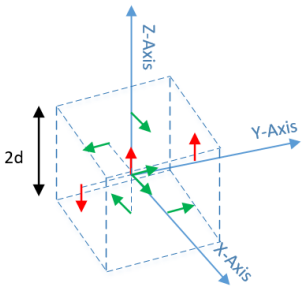

Figure 4. Configuration 1: 9 accelerometers. 3 in the origin and the 6 others arranged on the center of each face

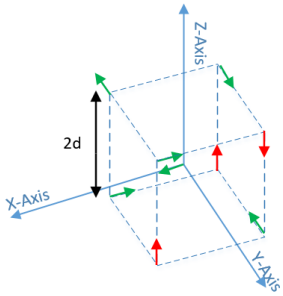

Figure 5. Configuration 2: 9 accelerometers. 1 in the origin and the 8 others arranged on each vertex

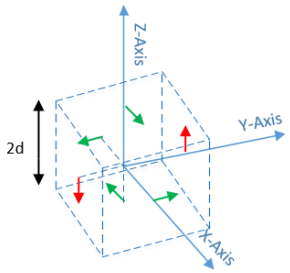

Figure 6. Configuration 3: 6 accelerometers. Arranged on the center of each face

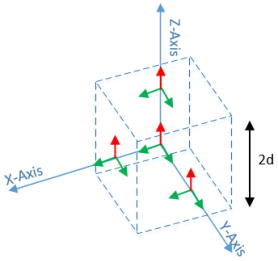

Figure 7. Configuration 4: 12 accelerometers. 1 triad in the origin and the other triads are on the center of 3 orthogonal faces

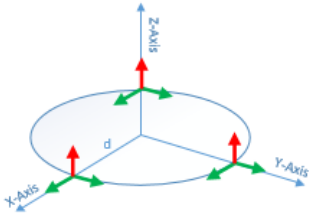

Figure 8. Configuration 5: 9 accelerometers. Arranged in 3 triads around a circle with radius d

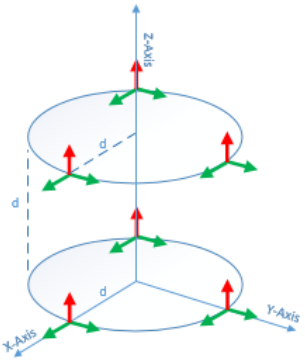

Figure 9. Configuration 6: 18 accelerometers. Arranged in 6 triads around 2 circles with radius d and a distance d between them

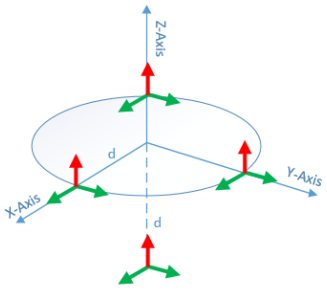

Figure 10. Configuration 7: 12 accelerometers. 9 arranged in 3 triads on a circle within radius d, another triad in on the z-axis at distance d from the origin

REFERENCES

[1] *Titterton, David, John L. Weston, and John Weston. Strapdown inertial navigation technology. Vol. 17. IET, 2004.*

[2] *Chin-Woo Tan, Sungsu Park, Krill Mostov, and Pravin Varaiya. "Design of Gyroscope-Free Navigation Systems". In Proceedings of the IEEE Intelligent Transportation Systems Conference, August 2001.*

[3] *C. W. Tan and S. Park, "Design of accelerometer based inertial navigation systems," Instrumentation and Measurement, IEEE Transactions on, vol. 54, pp. 2520-2530, 2005.*

[4] *A.R. Schuler, A. Grammatikos, and K.A. Fegley. "Measuring Rotational Motion with Linear Accelerometers". IEEE Transactions on Aerospace and Electronic Systems, Vol. AES-3, No. 3:465–471, 1967.*

[5] *Jeng-Heng Chen, Sou-Chen Lee, and Daniel B. DeBra. "Gyroscope Free Strapdown Inertial Measurement Unit by Six Linear Accelerometers". Journal of Guidance, Control, and Dynamics, Vol. 17, No. 2:286–290, March-April 1994.*

[6] *Hanson R., Using Multiple MEMS IMUs to Form a Distributed Inertial Measurement Unit, Master's Thesis, Air Force Institute of Technology, March 2005.*

[7] *Nusbaum U. and Klein I, Control Theoretic Approach to Gyro-Free Inertial Navigation Systems, IEEE AES Magazine special issue on navigation, August 2017, pp. 38-45, 2017.*

[8] *Optimal Gyro-Free IMU Geometry by Ryan Hanson, and Meir Pachter Air Force Institute of Technology AFIT/ENG Wright-Patterson AFB, OH, 45433*

[9] *I. Klein, "Analytic error assessment of gyro-free INS", Journal of Applied Geodesy, vol. 9, no. 1, pp. 49-62, 2015.*

[10] *A. K. Cline, C. B. Moler, G. W. Steward, and J. H. Wilkinson, "An estimate for the condition number of a matrix," SIAM J. Numerical Anal., vol. 16, no. 2, pp. 368–375, 1979.*

[11] *E. Vaknin, I. Klein, "Coarse leveling of gyro-free INS", Gyroscopy Navig., vol. 7, pp. 145-151, 2016.*

[12] *Z. C. Wu, Z. F. Wang, Y. Ge, "Gravity based online calibration for monolithic triaxial accelerometers' gain and offset drift", Proc. 4th World Congr. Intell. Control Autom. pp. 2171-2175, 2002.*